A New Series of Aerofoil Sections Suitable for Aircraft Propellers

A J BOCCI

(Aircraft Research Association)

Summary: A series of advanced aerofoil sections suitable for aircraft propellers has been developed. The sections combine advanced supercritical flow characteristics with good low-speed performance and are also directly applicable to other rotating aerodynamic machinery, such as low-solidity ducted fans, windmills, etc. The work has focused initially on propeller sections of around 6 per cent thickness/chord ratio, typical of the fundamental blade station where peak loading is usually carried (0.7 x radius). The complete section family covers a wide range of thickness/chord ratios, from 3 per cent to over 20 per cent. The profiles are defined by mathematical formulae and distort with thickness to achieve a shape having optimum performance characteristics at the flow conditions expected for that thickness. A subset of the family is defined for higher Mach number penetration, up to near sonic values. Practical applications of the new sections have shown notable gains.

1. Introduction

In the years since the Second World War considerable advances have taken place in aircraft wing design but, until now, comparable progress has not been made in the field of aircraft propellers. To remedy this, a series of advanced aerofoil sections suitable for propellers has been developed as a collaborative venture between the Aircraft Research Association Ltd and Dowty Rotol Ltd, the major manufacturer of the aircraft propellers in the United Kingdom.

An aircraft propeller generates thrust by imparting a change of momentum to the air passing through the disc, and this thrust varies according to the operating conditions of the aircraft. Usually the thrust requirements at specific operating conditions within the flight envelope are specified to the propeller designer by the airframe manufacturer, together with the engine power available and the associated rotational speed. The propeller designer is then concerned with producing a solution which meets the specified thrust requirements for a minimum weight and with sufficient structural safety margins.

An initial choice of the number of propeller blades, diameter and average chord is made, in the light of previous experience, by relating the power input to the propeller to the maximum output thrust required, subject to such constraints as ground clearance, noise levels and weight. A fairly standard radial distribution of thickness is initially assumed. For a metal-bladed propeller, for instance, a thickness/chord ratio of approximately 0.06 might be chosen on the main part of the blade, changing rapidly to a circular cross section towards the hub. The main limitation is the structural weight/strength compromise, although maximum blade Mach number can have some effect.

Performance calculations in the early stages may be conveniently executed using the method of Reference 1, in which performance is estimated by a semi-empirical means based on the 0.7 x radius blade section. From the blade section characteristics and input engine power, the performance at any flight condition may be estimated in terms of efficiency or thrust.

Assuming that the initial design looks satisfactory, a more detailed strip analysis approach can then be considered. Each radial position on the blade is considered as an isolated aerofoil element, with known two-dimensional characteristics of drag and lift over a range of incidence and Mach number. A typical velocity and force diagram for such an element, at some propeller operating condition, is shown in Figure 1. The main velocity field $(V,\omega r,W_0)$ is known from the operating condition and a velocity increment w is induced by the propeller operation. This inflow increment is shown

Received June 1976; revision received November 1976

https://doi.org/10.1017/S0001925900007939

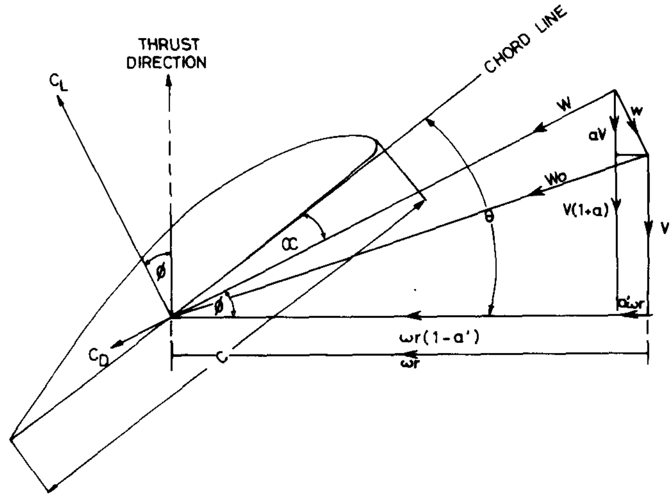

Figure 1 Velocity and force diagram, propeller blade element

in Figure 1 to have axial and rotational directions but, if it is assumed to be normal to the resultant incident flow W, i e, to be entirely lift-induced, then it is possible to produce an expression relating this inflow to the section C_L. The blade angle θ can then be obtained by comparing the C_L obtained from this expression with the curve of C_L against α. Repetition of this procedure for all stations on the blade defines a complete twist, and the C_L and C_D values lead directly to the forces on the blade elements, which can then be integrated to give the overall propeller thrust and torque. This process would normally be performed at the propeller design condition where efficiency, i e, the ratio of thrust to power input, is to be maximised. Changes can be made to the section or the initial design parameters and the process repeated to obtain optimisation. The complete twisted blade that results is then checked at other operating conditions to ensure that its performance is adequate.

Once an aerodynamic design has been finalised the blade elements, stacked about some suitable axis through, say, the centre of gravity of each element, then define a complete blade. This must be analysed to ensure that steady and vibratory stresses are acceptable, that natural frequencies are conveniently placed relative to the operating band of rotational speed and that the blade surface is smooth and can be manufactured by conventional means. Any changes required must be incorporated into subsequent design iterations.

Referring again to Figure 1, the thrust (δT) and torque (δQ) of the blade element may be incorporated into a standard expression for efficiency (e g, Reference 2):

$$\eta = \frac{V\,\delta T}{\omega\,\delta Q} = \frac{1-a'}{1+a}\tan\phi\,\frac{C_L\cos\phi - C_D\sin\phi}{C_L\sin\phi + C_D\cos\phi} = \frac{1-a'}{1+a}\,\frac{\tan\phi}{\tan(\phi+\gamma)},$$

where V is the free-stream velocity, ω the blade angular velocity, $a \times V$ is the axial velocity increment, a' is the rotational inflow, ϕ is the total flow direction relative to the plane of rotation, and $\tan\gamma = C_D/C_L$.

This formula shows that efficiency is automatically low when a is large and ϕ is small. This occurs at near-static conditions, i e, aircraft take-off, and in this situation large values of γ would significantly reduce efficiency. Thus, at the high values of C_L required to give sufficient thrust, high values of drag must be avoided and these can occur if the blade section is stalled. Conversely, at aircraft cruise conditions a is small, ϕ is larger* and relatively low values of lift/drag ratio on the blade sections can be tolerated before propeller efficiency is impaired very significantly.

Thus momentum considerations dictate the overall blade design, but the choice of sections depends on suitable aerodynamic properties. If, as is often the case, the blade is designed for static or fairly low forward speed conditions, then the thrust may be maximised, or blade size minimised for a given thrust, by operating at the maximum C_L compatible with good values of L/D, i e, sections are required for which the drag rise with C_L is delayed as far as possible.

It is necessary for manufacturing purposes to generate a smooth blade surface from the sections, which must also vary continuously in thickness and in centre of gravity position. In addition, for routine design purposes a wide range of sections of known aerodynamic characteristics must be available. These points are most easily met by a family of sections varying in some simple geometric fashion. Clark Y and NACA series 16 are examples of two families which have been used, the latter being preferred in post-war years since the farther aft position of the section maximum

* Clearly the magnitude of ϕ is constrained by considerations of propeller efficiency.

thickness is more compatible with the high propeller tip speeds which have been common (although lower tip speeds are expected in future, for noise reasons). C-4 sections form another series which have been used for ducted fans. Sections within the NACA series 16 family vary linearly in thickness and camber separately. Experimental results are available from early transition-free NACA tests, giving section lift and drag for a wide range of incidences and Mach numbers for various sections within the family.

There is considerable variation in local Mach number, both along a propeller blade at any given operating condition and also between operating conditions. The latter variation is illustrated by Table I, which represents the operating conditions at station 0.7, i e, the station at 0.7 x radius on a typical sample blade. In general, the Mach number can vary from very low values near the hub to near-sonic values at the tip in some cases. It would be surprising if a family of sections varying in such a simple geometric fashion as NACA series 16 could perform well over a wide range of Mach numbers. Accordingly, some investigations were initiated to see whether improvements could be made to a standard NACA series 16 aerofoil in the light of present-day aerodynamic knowledge. These have led to successful aerofoil section experimental tests. A new family of aerofoil sections has been developed, related by simple mathematical formulae. The sections, as will be seen later, offer a very high level of aerodynamic efficiency giving, in many applications, substantial gains in performance.

TABLE I

Operating Conditions at 0.7 Radius on a Propeller Blade

(C_D values for NACA series 16 sections assumed)

	M	C_L	C_D
Take-off	0.49	1.25	0.045
	0.50	1.05	0.012
	0.52	0.82	0.007
Climb	0.53	0.58	0.008
Normal cruise	0.60	0.46	0.011
High-speed cruise	0.69	0.34	0.017

The work described has been undertaken at ARA in close collaboration with Dowty Rotol, the company providing the financial support and specifying the design requirements and practical constraints to be expected. The design procedure which has been used by the company starts with the choice of suitable sections from the NACA series 16 family which are applied, using their known aerodynamic characteristics, in a similar manner to that already outlined. In describing the development of the new sections, we shall be concerned with essentially two-dimensional characteristics, assuming that these carry across to the true situation of dynamic flow on the rotating propeller. This is known to be broadly true but some changes must be expected, although their nature is arguable.

So far the discussion has concerned propellers, but it should not be forgotten that the section performance is equally relevant to any rotating aerodynamic machinery, such as low-solidity ducted fans, windmills, etc. In higher-solidity cases such as turbines, a cascade effect comes into play in which pressures on the blades are influenced by their proximity, but the isolated section characteristics are of some importance and the changes to be discussed here are still relevant.

In the next section the aerodynamic limitations of a typical NACA series 16 aerofoil are analysed. Then the design of a new aerofoil to a specified set of requirements is described and its broad performance characteristics given. The way in which this is extended to a complete family of aerofoils, covering all thicknesses, is then indicated. Further test results on other sections within the family are then discussed, and finally some examples of potential and actual applications of sections to propellers and ducted fans are given.

Notation

V	free-stream velocity
ω	angular velocity
r	blade element radius

W_0	blade element onset flow field component
w	velocity increment induced by propeller rotation
W	blade element total flow field component
θ	blade element geometric incidence setting
α	blade element incidence relative to total flow field, or two-dimensional wing section incidence relative to free stream
ϕ	flow direction relative to plane of rotation
C_L	lift coefficient
C_D	drag coefficient
C_m	pitching moment
L/D	lift/drag ratio, $\equiv C_L/C_D$
γ	defined by $\tan\gamma = C_D/C_L$
δT	blade element thrust
δQ	blade element torque
η	blade element efficiency
a	axial velocity increment, fraction of free stream
a′	rotational inflow increment, fraction of radial velocity
M	Mach number
Re	Reynolds number
c	section chord length
t/c	section thickness/chord ratio
x/c	non-dimensional distance along chord
z/c	non-dimensional section ordinate
z_t/c	non-dimensional section thickness
z_s/c	non-dimensional section camber

2. Conventional Blade Section

It is convenient to discuss the limitations of NACA series 16 sections in the context of the sample strip-analysis data in Table I. This applies to station 0.7, the fundamental design station, at which the loading peak along the blade occurs. The data are based on the performance characteristics of a NACA series 16 section of 6 per cent thickness/chord ratio and with a "design C_L" of 0.716. It is apparent that the data can be broadly divided into low Mach number (about $M = 0.5$) take-off and climb conditions, and higher Mach number cruise conditions. To consider the data in more detail we would wish to examine experimental results on the section. However, recent test results in a modern tunnel are available only for a 6 per cent thickness/chord ratio NACA series 16 section with a design C_L of 0.5, corresponding to a lower camber having a maximum value of 2.8 per cent of the chord. The section was tested in the ARA 18 in x 8 in (457 mm x 203 mm) two-dimensional tunnel, the tests being conducted transition-free, and at a chord Reynolds number of 4.5×10^6. Both maximum thickness and maximum camber on this series of sections are at $x/c = 0.5$, and the geometry is shown in Figure 2(a). The section is, in fact, not quite standard compared with the NACA series 16, since the trailing edge is thickened and rounded, for ease of manufacture on a propeller. The small leading edge radius is apparent.

Returning to the strip-analysis data in Table I, it can be seen that at take-off conditions drag is appreciable for higher values of lift, $C_L \geqslant 1.0$, and the reason for this can be seen by examining the experimental results for the section tested.

The variation of lift with incidence and drag with lift are included in Figure 3 and we are concerned for the moment with the $M = 0.5$ case. For this Mach number flow development through the stall is illustrated by pressure distributions at $\alpha = 6°, 8°, 10°, 12°$ and $14°$ in Figure 4(a). The pressure distributions at $\alpha = 6°$ and $8°$ show a

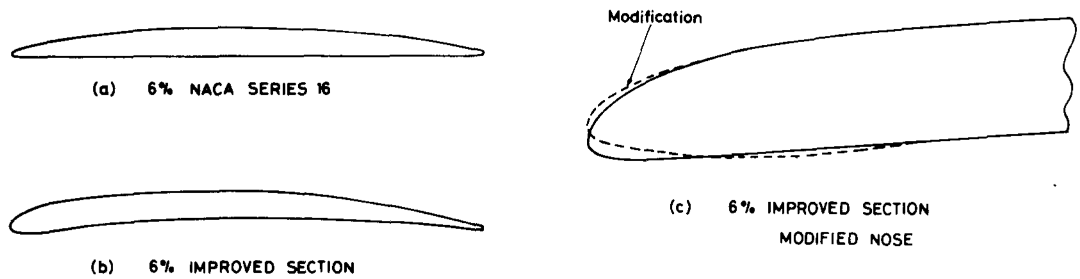

Figure 2 Section geometries

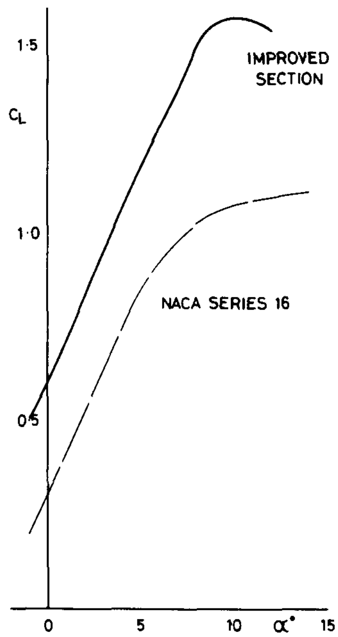

Figure 3(a) Lift curves, $M = 0.5$

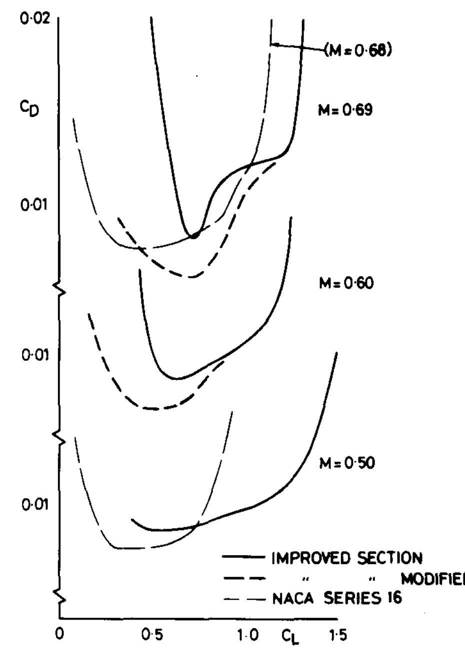

Figure 3(b) Drag curves

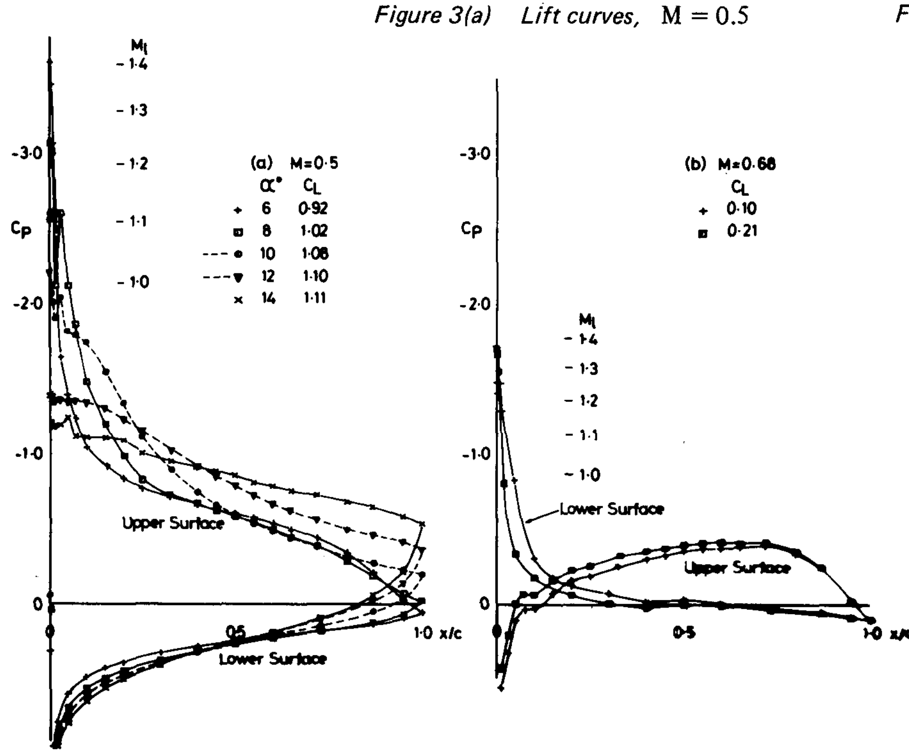

Figure 4 6 per cent NACA series 16, pressure distributions

sharp leading-edge suction peak followed by a separated region, which spreads back towards the trailing edge with increasing incidence, so that there is a complete detachment of the flow on the upper surface after about $\alpha = 10°$. Examination of schlieren photographs, not presented here, showed that the flow is extensively separated on the upper surface at $\alpha = 8°$. A feature of the results is the fact that lift (as calculated from integrated pressure distributions), continues to increase well beyond $\alpha = 8°$ and, in fact, maximum lift is achieved at $\alpha = 14°$, although the flow is possibly significantly three-dimensional. Incidentally such levels are often assumed in propeller design calculations, and are implied by thrust values which have been achieved on propellers in the past.

Consider now the Mach number 0.68, for which the drag variation with lift and the pressure distributions at representative values of C_L are shown in Figures 3(b) and 4(b). At the high-speed cruise point on the more highly cambered section in Table I, a relatively high drag is expected. Figure 3(b) shows that drag is not a problem with the tested section at $C_L \simeq 0.4$, but it increases rapidly at lower incidences owing to the growth of a shock-induced separation bubble on the lower-surface leading edge, as indicated by the pressure distributions in Figure 4(b). This is the source of the drag quoted in Table I.

It appears, therefore, that NACA series 16 sections have reduced efficiency at higher values of lift at low Mach numbers, owing to the excess drag produced by the leading-edge flow separation. The drag rise can be delayed to higher values of C_L by some increase of camber. However, the drag rise, when it occurs, is rapid and implies peak values of L/D over a narrow C_L band, which cannot necessarily be utilised fully in a propeller design. There is also the limitation on the camber of the need to achieve low values of C_L at higher Mach number cruise conditions.

The performance points quoted in Table I are fairly representative, although significant variations occur between propellers and, in addition, Mach number varies appreciably across the blade. Figure 6 shows that the section is performing more satisfactorily at high lift when considered as a tip section operating at about $M = 0.65$. However, this applies only to a narrow Mach number band and, in particular, the low Mach number performance of NACA series 16 sections clearly leaves something to be desired. It will become apparent that the new section family finally defined shows, in many cases, appreciable improvements over the whole Mach number range.

3. An Improved Blade Section

It is worth listing the target requirements of an improved section, suitable for a research exercise as originally suggested to ARA. The section should be of thickness/chord ratio 0.06 and should have:

(a) A finite trailing-edge radius or thickness; radius $>$ 0.2 per cent chord preferably.

(b) As large a leading-edge radius as possible without compromising the design.

(c) No concavity on the suction surface.

(d) Preferably no concavity on the lower surface; certainly no local concavity (i e, extending over less than 20 per cent chord).

(e) A gentle stall. (Little or no loss of C_L at incidences above that for $C_{L\,max}$.)

(f) A wide range of C_L for good lift/drag ratios (biased towards high C_L rather than low), rather than an exceptional L/D for a narrow range of C_L.

(g) Maximum $C_L \geqslant 1.6$ at $M = 0.5$.

(h) A low pitching-moment coefficient, C_m, relative to the section centre of gravity at low and negative values of C_L.

Points (a) – (d) are concerned with propeller manufacture. The minimum trailing edge thickness in (a) presents no problem and, in fact, modern aerofoil sections use this feature as a means of alleviating boundary-layer rear separation problems, although they are not usually faired off to produce a radius. Similarly, the bluff leading-edge requirement (b) is a modern feature which should help the design of good low-speed qualities into the section. In practice, it would aid the fitting of leading-edge protective devices. Points (c) and (d) are imposed so that the firm's standard practice of using sanding discs in the later stages of blade production can be retained. Point (c) removes the option of designing to the limit of boundary-layer separation over a significant portion of the upper surface, which is probably too risky in any case. The lower surface limitation (d) has been relaxed to a somewhat nominal minimum radius of about 1300 mm. With a chord of 300 mm (typical of many propeller blades) such a lower-surface shape conveniently results in the degree of camber found to be desirable for an improved section. It is assumed that any further curvature increase, associated with moderate change of camber or chord, would not present significant manufacturing problems.

Points (e) – (h) are aerodynamic requirements. In fact NACA series 16 sections already apparently possess feature (e) at $M = 0.5$, as described earlier, although it is also associated with rear-separation characteristics. The latter approach is adopted here. Requirement (f) implies that increases in C_L should be associated with progressive moderate increases in drag, as would be expected from a rear separation. Point (g) is related to (e) in that the firm uses performance estimates for NACA series 16 sections in which it is assumed that lift continues to increase with incidence beyond the stall, reaching and maintaining a level referred to as $C_{L\,max}$. This propeller behaviour contrasts with the situation in two-dimensional experimental tests in which the lift usually drops after the stall, although this is apparently delayed appreciably for long bubble-type separations, as already discussed. Here we aim to achieve as high a lift as possible at $M = 0.5$ in experimental tests on the section, and we assume that some further favourable effects would be expected on a propeller. Requirement (h) is perhaps of less importance and in any case is difficult to use as a design parameter without seriously compromising the design.

In developing an improved section the Bauer, Garabedian and Korn (G + K)[3] computer programme, with the geometry mapping replaced by that of Sells[4], was used to calculate supercritical flows occurring, mostly, near the leading edge. For general subcritical viscous calculations, to determine the main characteristics of pressure distributions and forces (for attached flows), the Powell programme[5] with Horton's boundary-layer method[6] was found to be acceptable in the present context.

A section was designed, using these computer programmes, and then manufactured as a 152 mm chord aerofoil and tested in the ARA 18 in x 18 in (457 mm x 203 mm) two-dimensional tunnel. As with the NACA series 16 aerofoil, the experiment was conducted transition-free, and at a Reynolds number of 3.5×10^6 .

The section geometry is shown in Figure 2(b). A thickness of 0.06 chord is maintained from near the leading edge to the mid-chord region and is then tapered off to a trailing-edge thickness of 0.005 chord. There is significant camber, with a somewhat drooped leading edge, giving a high curvature region or "corner" at around 0.1 chord followed by a relatively flat region on the upper surface, and a lower surface with fairly uniform curvature distribution, for ease of manufacture. The leading edge is much more bluff than for the NACA series 16 aerofoil shown in Figure 2(a), but it has the particular feature of a parabolic shape such that the precise leading-edge radius is small relative to the rate of growth of thickness immediately aft. This is an important feature, giving a local curvature distribution to produce an appropriate supercritical flow when the terminating shock occurs close to the leading edge, at high lift at Mach numbers at and below about 0.5. It also determines the way in which the leading edge blends in to the lower surface, which is relevant to the achievement of cruise conditions with high Mach number and low C_L , but which was not one of the design requirements for the present section. The geometry modification shown in Figure 2(c) was introduced for such reasons and is discussed later.

The development of the stall in the experimental tests at $M = 0.5$ and $M = 0.69$ on the new section is shown by the pressure distributions in Figure 5; lift curves at $M = 0.5$ are included in Figure 3(a) and drag variation with lift in Figure 3(b). If pressures at $M = 0.5$ in Figure 5(a) are compared with the NACA series 16 pressure distributions in Figure 4(a), a dramatic change in stalling characteristics is observed. The leading-edge long bubble separation has been exchanged for a progressive trailing-edge stall to give much higher values of $C_{L\,max}$, as shown by the lift curves in Figure 3(a). The leading-edge shock interacts with a laminar boundary layer and thickens the layer, but has been kept to a minimal strength and terminates a broad suction peak. Tests to determine the effect of moving boundary-layer transition ahead of the shock, by using leading-edge roughness, suggested that the laminar interaction was only a minor factor in the effectiveness of the design. The pressure distributions at $M = 0.69$ in Figure 5(b) show that the "corner" at 0.1 chord on the upper surface generates a suction peak from which the flow tends to recompress, unlike the situation at $M = 0.5$ where the supercritical region is almost entirely ahead of the corner. The main shock rapidly moves aft with increasing incidence but remains relatively weak, giving a high maximum lift from the supercritical suction region. Furthermore, the supercritical pressure distribution is not sufficiently peaky to prevent transition moving aft with the shock, with a favourable effect on the boundary-layer thickness and thus on the maximum lift

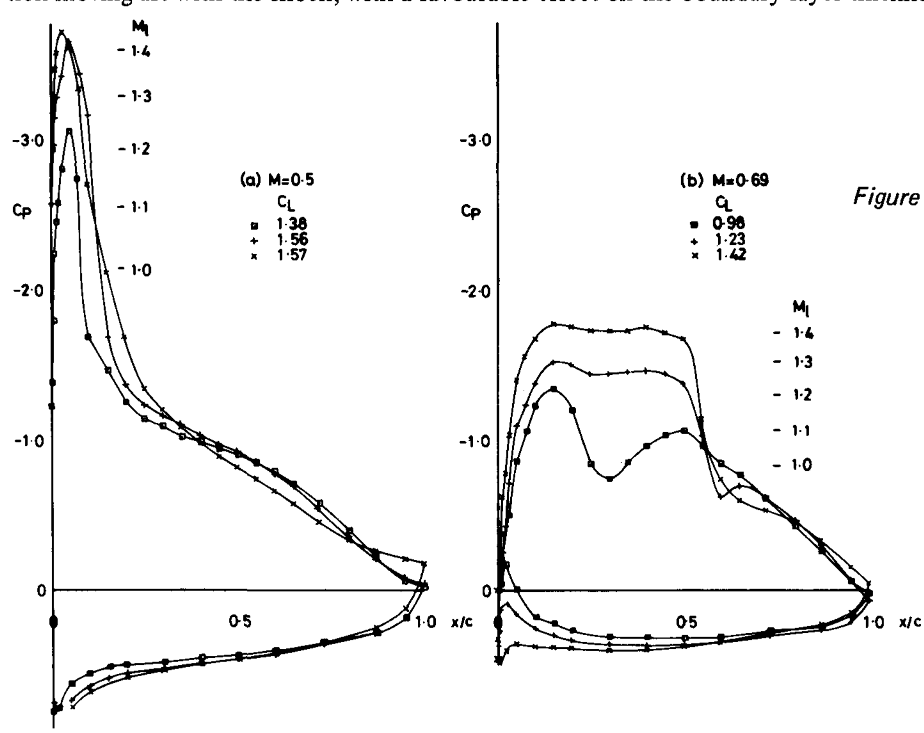

Figure 5 6 per cent improved section, pressure distributions

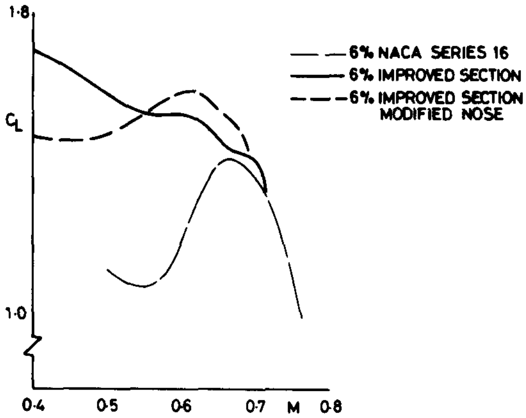

Figure 6 $C_{L\,max}$ *boundaries*

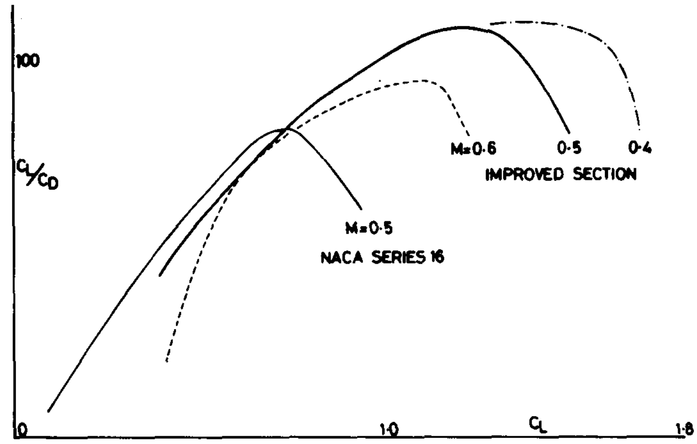

Figure 7 Lift/drag curves

Figure 8 6 per cent improved section, pressures. Effect of modified nose

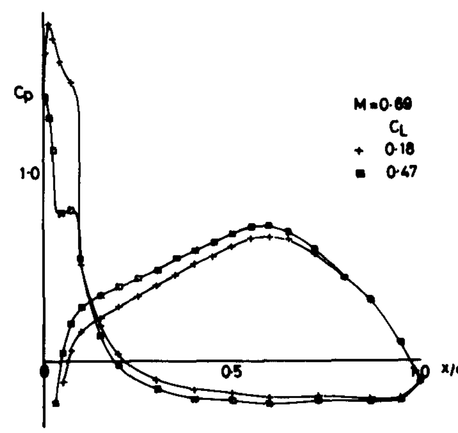

and drag achieved. The maximum lift boundary is compared in Figure 6 with that of the NACA series 16 section already tested and it can be seen that the new section also performs well at other Mach numbers. It appears that optimising upper-surface shock growth and carrying sufficient camber, so that the adverse effects of the shock and the rear boundary-layer thickening tend to occur at roughly the same incidence, has paid dividends in that high C_L has been achieved over a wide Mach number range while the flow remains relatively well behaved.

Figure 3(b) shows that basic drag levels for both sections are quite low and this may be ascribed not only to the small thickness/chord ratio (0.06) of the sections but also to the aft transition positions which occur. On a propeller even lower blade section drags are often expected. These are believed to be due to a centrifugal "scouring effect".

The section geometry shown in Figure 2 and the experimental results given in Figures 3, 5 and 6 indicate that the requirements for an improved section interpreted from the listed requirements (a)–(h) have been met. Curves of lift/drag ratio, a measure of section efficiency, are given in Figure 7 for a range of Mach numbers and the improvement at $M = 0.5$ over the NACA series 16 section, results for which are also shown, is striking.

So far we have considered the performance of the new section relative only to the original design requirements in which the emphasis lay in achieving high C_L at static conditions. In fact, as already outlined, the section achieves high C_L for a wide range of Mach numbers. However, reference to Table I shows that, in that example, a static Mach number of 0.5 is associated with cruise Mach numbers of 0.6 and 0.69 for quite low C_L, and such relative values are fairly typical of what could be expected in aircraft applications. Examination of the drag curves for the new section at the higher Mach numbers in Figure 3(b) show that the drag characteristics are poor at low values of C_L and this can also be seen in the lift/drag curve for $M = 0.6$ in Figure 7. The degradation in performance is due to a shock-induced separation bubble on the leading-edge lower surface. The geometry in the nose region was modified as shown in Figure 2 and the new shape was tested in the ARA two-dimensional tunnel. Experimental pressure distributions are shown in Figure 8 and drag variation with C_L is included in Figure 3(b). The supercritical flow on the leading-edge lower surface now recompresses satisfactorily to the shock and consequently the drag characteristics have been greatly improved, now lying within $\Delta C_L \simeq 0.1$ of the original NACA series 16 section, in spite of considerably greater camber, However, Figure 6 shows that the good high-lift performance of the original section has been degraded somewhat below $M = 0.55$ but improved in this respect at higher Mach numbers, in both cases because of the slightly more peaky nature of the section.

It appeared possible to develop the section shape further, to achieve the good low-C_L drag characteristics without compromising the high-lift performance, but it was felt that the research exercise had yielded sufficient information to proceed to the definition of a section family with some confidence.

4. A New Section Family: The ARA-D Series

So far, sections of 6 per cent thickness/chord ratio with fairly specific operating points have been discussed, but for practical purposes it is necessary to define sections covering a wide range of thickness and operating conditions.

Such a section family has been developed within the practical constraints already specified. The range of possible thicknesses and operating conditions which was used as guidance is shown in Figure 9, grouped for illustrative purposes to show the maximum variation in each blade region. The Reynolds number limits shown relate only loosely to Mach number, since blade chord and operating altitude are obviously important factors.

Figure 9 shows that the root sections and inboard sections, groups (1) and (2), have an extreme range of thickness/chord ratio but quite low operating Mach numbers and Reynolds numbers, by full-scale aircraft standards. The implication is that compressibility effects can be practically ignored but that rear boundary-layer separation characteristics are an important factor. For the outboard sections, group (3), compressibility effects are starting to become important and the characteristics of the improved section already discussed are directly relevant, although Reynolds numbers could well be lower than that (3.5×10^6) at which the section was tested and found to be quite close to rear separation under many conditions.

The tip sections, group (4), were originally limited in Figure 9 to $M = 0.8$, since it was felt that lower tip speeds were likely in future for noise reasons. However, the favourable supercritical flow characteristics already shown for the improved section will be seen to carry across to the thinner tip sections. These should operate very well up to near-sonic speeds, although the ARA two-dimensional tunnel and, to a lesser extent, converged theoretical solutions, are at present limited to about $M = 0.85$ and so the higher Mach number section characteristics are more uncertain.

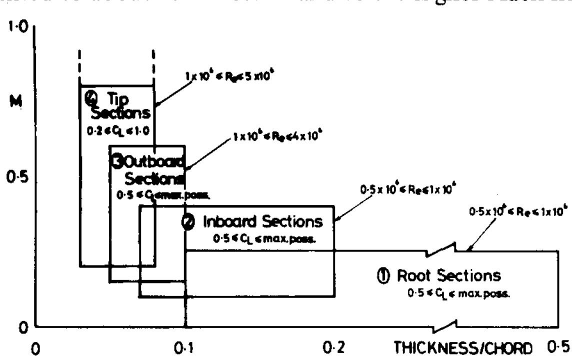

Figure 9 Thickness and performance range

The range of requirements in Figure 9 must be interpreted realistically. For example, the thicker sections in a group are less likely to operate at the higher Mach numbers in that group. Conversely, the thinner sections could operate at any Mach number within the group, including the lowest. For applications which operate nearly or entirely in static conditions, such as hovercraft propellers or low speed fans, maximum C_L is usually required at relatively low Mach numbers. In other cases, such as aircraft propellers, the high C_L static condition would be coupled with a lower C_L requirement occurring at some Mach number greater than static, perhaps by a margin of $\Delta M = 0.1$ or even 0.2, e g, Table I. Thus the highest Mach number within a group is taken to correspond to the lowest C_L for some maximum drag rise, say $\Delta C_D = 0.010$, acceptable for cruise conditions.

It happens that sections belonging to groups (1), (2) and (3) which essentially satisfy the performance requirements may be defined uniquely for a given thickness. However, the geometry of a thin section belonging to group (4) suitable for a low-Mach-number/high-C_L static case would be inappropriate to high-Mach-number/low-C_L cruise conditions. This is because the high camber necessary for the former, limited only by considerations of rear flow separation, would have high curvature on the lower-surface leading edge, giving rise to extreme suction peaks and excessive levels of drag in the cruise condition. Some camber constraint must be applied. In addition, the geometric nose modification applied to the original 6 per cent thickness/chord section is incorporated to some extent as a feature of the section family.

At this stage it is worth emphasising the importance of the outboard sections, group (3). These typically carry the main part of the blade load, as compared to the thick sections near the hub which provide very little thrust, and the very thin tip sections which tend to be somewhat off-loaded (as indicated in Figure 9). The basis of the section family is the 6 per cent thickness/chord improved section already discussed, although the shape is changed slightly as described later. With increasing thickness the shape distorts to maintain the best possible rear boundary-layer attachment characteristics, while with reducing thickness the camber constraint may be applied to give suitable Mach number penetration.

The section family is described by simple analytical mathematical formulae. This is necessary to give the smooth surfaces necessary for high Mach number cases with supercritical flow regions, a continuous variation from section to section for radial surface continuity, and continuity of aerodynamic properties. Also, any section from an infinite family may be easily generated without the interpolation necessary from a finite number. Sections are defined by thickness and camber separately, with ordinates taken normal to the chord line; because the formulae describe shapes with continuous curvature, these may be combined directly to give smooth upper and lower surfaces. The way in which the thickness and camber forms are built up is shown in the sketch in Figure 10.

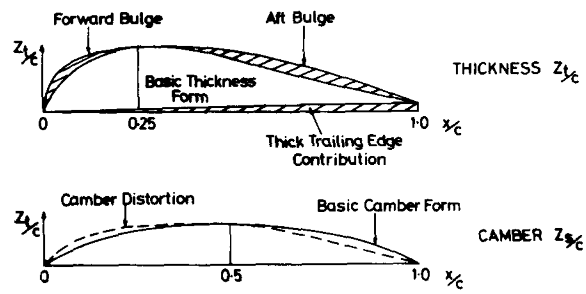

Figure 10 Geometric structure of section family

The sections are nominally defined from 3 per cent to 20 per cent thickness/chord ratio. It is impossible here to discuss all the considerations which have gone into the development of the variation of section geometry and only the main features will be given.

The basic thickness form reaches a maximum at $x/c = 0.25$ and is parabolic at the leading edge and cusped at the rear. The forward bulge is the most important feature of the sections. It has the same parabolic shape at the leading edge as the basic thickness form and this is a fundamental feature of the sections, contrasting with the more usual circular shape. The rapid increase in thickness on moving away from the leading edge, owing to the parabolic shape, is followed by the bulge blending in to the basic thickness form at $x/c = 0.25$, resulting in a high curvature region near $x/c = 0.1$ followed by a relatively flat surface. The aft bulge also gives a flatter surface, as well as providing sufficient structural strength for the thinner sections. The forward and aft bulges are zero at the limit of zero section thickness, grow initially with thickness at roughly the same rate as the basic thickness form, to provide the flat surface characteristic for the thinner sections, and are again zero at the limit of 20 per cent thickness/chord ratio. All sections have relatively thick bases, for example 1 per cent for 5 per cent thickness/chord ratio and 2.5 per cent for 20 per cent thickness/chord ratio, and this is incorporated in the thickness form as a simple wedge. The basic camber form is simply a parabolic arc symmetric about the mid-chord point and varying with thickness. For the thinner sections the net result with increasing thickness is that material is predominantly added to the lower surface. For the thicker sections the camber reaches a minimum at 20 per cent thickness/chord ratio, with this minimum camber line used for the even thicker hub sections. The camber distortion has a parabolic form near the leading edge, grows with thickness to maintain minimum aft upper surface curvature for the thicker sections, and retains an approximately constant leading-edge camber angle. It is important to state that the thickness and camber form, and thus the total profile shape of the basic family, is defined once and for all on specifying the thickness/chord ratio.

A selection from the basic family, of thickness/chord ratio 3 per cent, 6 per cent, 10 per cent and 20 per cent, covering the complete range is shown in Figure 11, with the thinner sections repeated, nesting inside the 20 per cent sections, to indicate the progressive shape changes involved. The 6 per cent section is in most respects very similar to the original improved section already discussed, except that the base thickness is greater and the aft upper surface curvature lower, to give boundary-layer attachment characteristics more appropriate to the generally lower Reynolds numbers of Figure 9. Also, the effect of the forward thickness bulge has been to give a suitable leading-edge lower-surface shape for good cruise performance, going some way towards the modification shown in Figure 2(c). In other respects the upper surface, with the high curvature at $x/c = 0.1$ produced by the forward thickness bulge and followed by a relatively flat region, results in a favourable supercritical flow development generally similar to that on the original section. The change from 6 per cent to 3 per cent thickness/chord ratio shows the removal of thickness predominantly from the lower surface, the matching of the aft upper surface, and the similar leading edge camber angle giving balanced emphasis to minimising peak suction and shock growth on the upper surface in static conditions and on the lower surface in cruise conditions. In static conditions at low Mach number the more peaky nature of the 3 per cent, compared to the 6 per cent, section is compensated by the higher basic section loading due to the camber. In cruise conditions at higher Mach number such thin sections would normally require reduced camber, as described later, and the corresponding static Mach number would often be sufficiently high that the more peaky nature of the section is no disadvantage, This effect was demonstrated by the nose modification to the improved section, Figure 2(c), which gave improved $C_{L\,max}$ for Mach numbers $\geqslant 0.55$ (Figure 6). The change from 6 per cent to 10 per cent thickness/chord ratio again shows the change in thickness predominantly on the lower surface and the matching of the aft upper surface. The upper-surface crest is further forward than on the thinner sections, to minimise leading-edge peaks and rear-separation tendencies at the low Mach numbers and Reynolds numbers likely for such thicker sections (Figure 9). The increasing thickness on the lower surface eases the leading-edge curvature, to reduce the likelihood of extreme peak suctions as well as reducing basic section loading, and means that there is no problem in meeting cruise requirements. The 20 per cent thickness/chord section shows that, on the upper surface, the crest is much farther forward towards the leading edge and the aft region is very flat to the thick trailing-edge base, again in the interest of minimising rear boundary-layer separation tendencies. The basic section family, uniquely defined once thickness is specified, forms a continuous variation between the profiles shown in Figure 11. The new section family is known as the ARA-D series.

A subset of the family is defined by reducing a camber factor below unity. The reduced camber may be necessary for aerodynamic reasons, particularly for the higher Mach number tip sections, or for some structural or other reason. The extreme case of the 3 per cent section (Figure 11) is an example which is very satisfactory for high C_L static cases but it is unable to achieve less than $C_L \simeq 1.0$ without a considerable increase in drag due to suction peaks on the lower-surface leading edge. Also, high Mach number penetration is limited by upper-surface curvature. Paradoxically the thicker tip sections of group (4) (Figure 9) are, up to a point, less constrained in these respects, since the lower-surface leading edge is locally much less curved and the farther forward crest position tends to flatten the upper surface. However, the thinner sections would obviously be necessary for very high Mach number penetration. The camber factor is chosen so that a required cruise condition may be achieved, smaller values generally being needed for the thinner than for the thicker sections, for the reason given. A factor, normally unity, is applied to the forward bulge which reduces with the camber factor and section thickness. This is necessary to counteract the tendency for the curvature of the lower-surface leading edge to increase with reducing camber, particularly on the thicker tip sections, resulting in stronger local shocks.

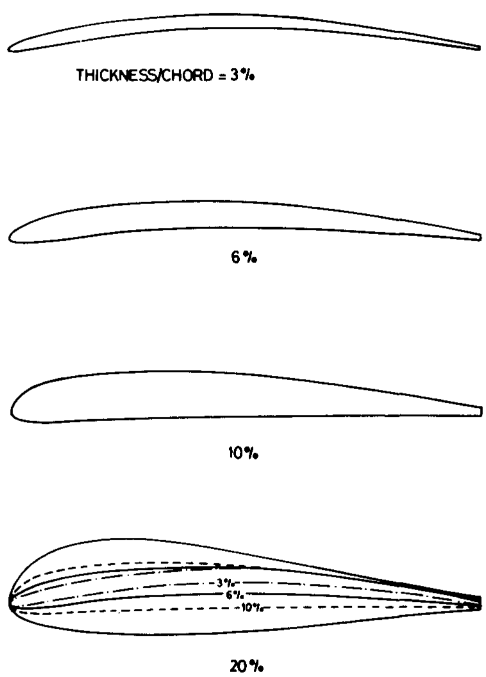

Figure 11 Profiles of section family

Having defined the section family it is necessary for design purposes to know the performance of any particular section, over at least the range suggested in Figure 9, in terms of lift, drag and pitching-moment curves. A continuing series of tests is being conducted in the ARA two-dimensional tunnel on selected sections, to construct a comprehensive set of data. The theoretical methods can be used to some extent in this process, mainly to interpolate for sections intermediate between those tested. The experiments are particularly necessary to establish the performance near boundaries of lift and drag, where significant flow separations and/or strong shocks are present. In fact it is frequently found that a blade is required to operate in off-design conditions at incidences well beyond those corresponding to the boundaries in two-dimensional tests and where the flow is probably largely three-dimensional. Some technique is usually adopted to produce extrapolations of the tunnel data which are plausible in the light of thrust values achieved on propellers in the past, but we shall not discuss this further here.

We shall consider two sections for which experimental results are available. A 13 per cent thickness/chord section was chosen to be representative of the inboard sections, group (2) of Figure 9. This was tested over an appropriate low Mach number range at Reynolds numbers of about 1×10^6. A 4 per cent thickness/chord section with a camber factor of 0.5 was chosen to be representative of the higher Mach number tip sections, group (4) of Figure 9. This was tested over a wide range of Mach numbers at Reynolds numbers of about 3×10^6.

The geometry of the 13 per cent thickness/chord section is shown in Figure 12, together with a summary of the performance characteristics. It can be seen that, considering the low Reynolds number, high values of $C_{L\,max}$ are achieved at $M = 0.3$ and 0.4. The pressure distributions show that this is due to a large contribution from the well-

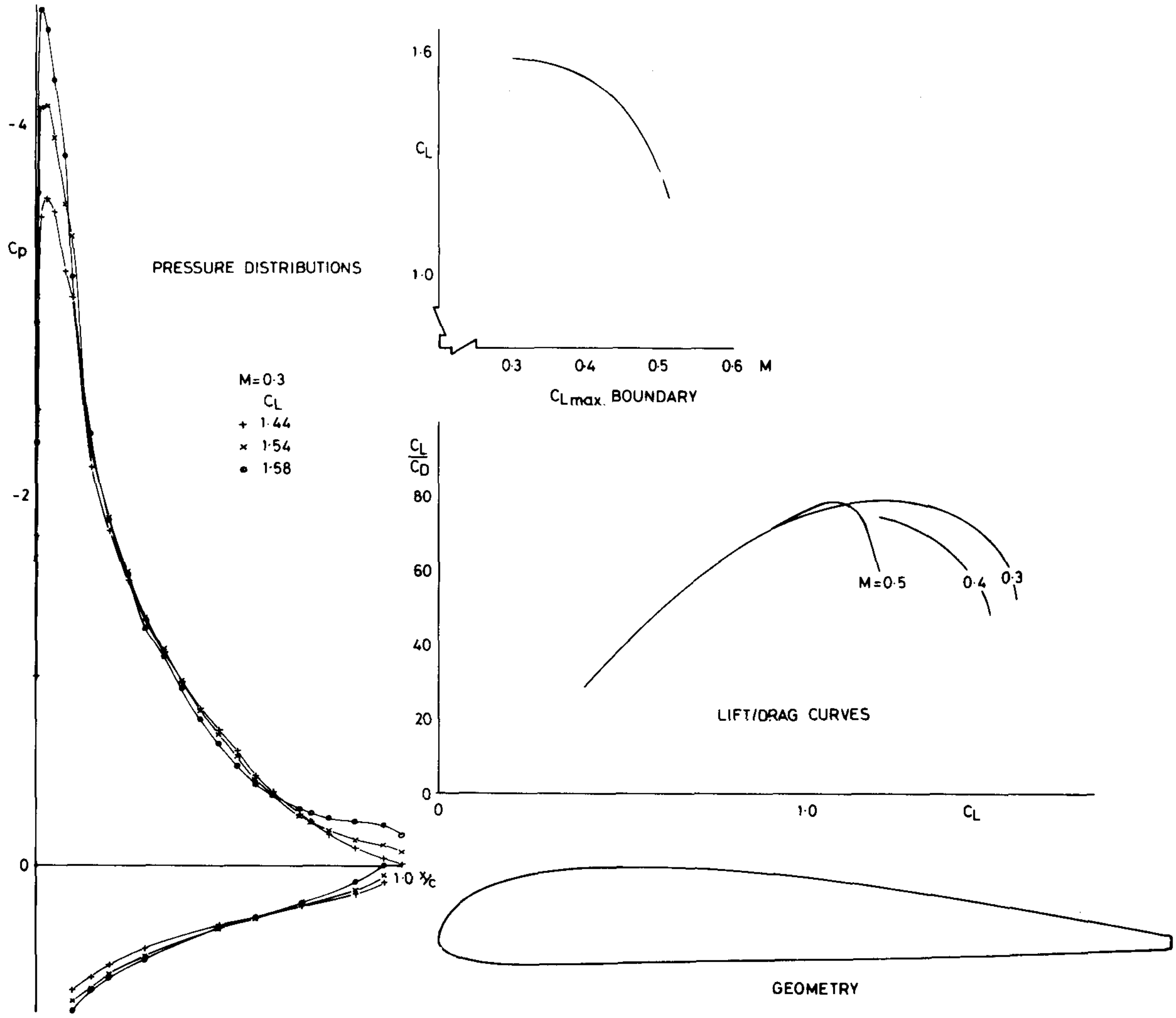

Figure 12 13 per cent section

spread peak suction region and a relaxing pressure gradient on the upper surface which delays trailing-edge separation. The lift/drag curves show that the section can be operated satisfactorily up to high values of C_L, failing to match those of the 6 per cent thickness/chord improved section in Figure 7 only because of the appreciable increase in thickness. Tests on a more highly cambered version of the 13 per cent section have given even greater values of $C_{L\,max}$.

The geometry of the 4 per cent thickness/chord section is shown in Figure 13, with a summary of the performance characteristics. We consider the high lift performance first. The pressure distributions at $M = 0.7$ show the characteristic peak suction at 0.1 x chord, followed by a supercritical recompression such that the shock strength sufficient to induce flow separation is delayed to a high C_L. The performance is clearly very satisfactory in the intermediate Mach number range. This might correspond, in practice, to the static condition for such a section. The pressure distributions at $M = 0.8$ show the development of an almost full-chord supercritical region with a pressure distribution sufficiently favourable to allow transition to occur, at the shock position. The combined effect is to give a very high value of $C_{L\,max}$ for such a Mach number. This is a situation in which forward transition fixing degraded the maximum lift by $\Delta C_L \simeq 0.15$, although a good value was still achieved. Of course, such a combination of high Mach number and lift is less likely in practice. Relatively high values of $C_{L\,max}$ are thus attained at the intermediate and high Mach numbers, with quite satisfactory values at the lower Mach numbers, considering the moderate camber and the small leading edge radius inevitably associated with such a thin section.

Consider next the Mach number penetration of the section. The drag boundary is probably representative of a maximum cruise limit. The pressure distribution at $M = 0.84$, $C_L = 0.22$, is close to the drag boundary and might, for example, represent a cruise point which could link with an intermediate Mach number static condition. The pressure distribution shows the features which enable the Mach number penetration to be achieved at such a low C_L. The leading-edge lower-surface peak suction region is well spread, to help to achieve the low C_L. The suction region is terminated by a shock which is weakened by the supercritical recompression. The expansion on the upper surface results in aft transition, but does not give a shock of sufficient strength to degrade the section performance.

Generally the section has good high-lift characteristics at all Mach numbers and good Mach number penetration for a wide range of lift. Thus, although the geometry is most suited to flow situations for which the section could well be

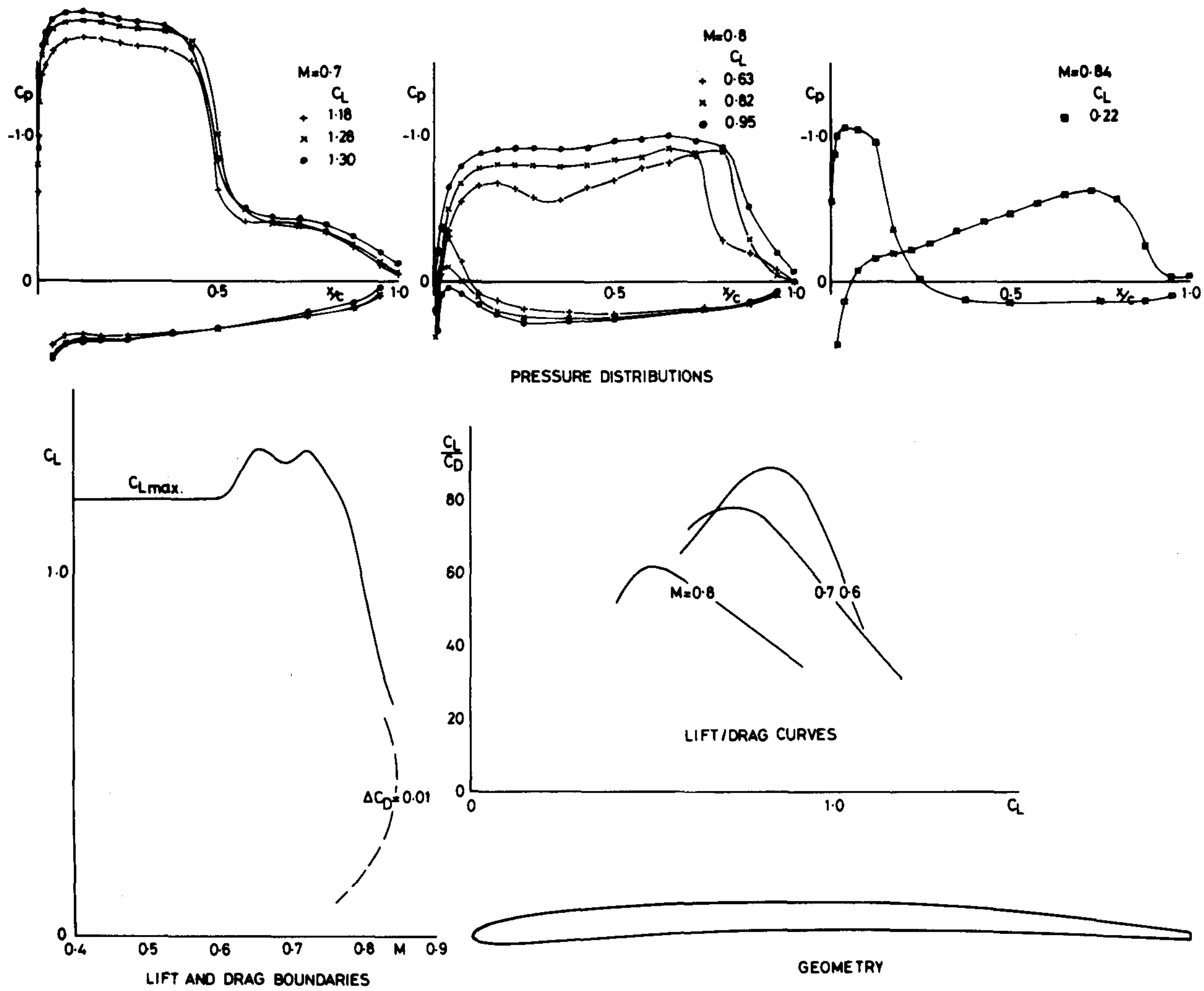

Figure 13   4 per cent section

chosen, it is also satisfactory in many other conditions. In contrast, NACA series 16 sections are limited in Mach number penetration by strong shocks caused by upper surface curvature. For this reason the high-lift performance is somewhat unsatisfactory at high Mach numbers as well as low, reaching a peak for a narrow intermediate Mach number band, as shown in Figure 6. At the other extreme, supercritical sections currently in vogue for aircraft wing applications are not generally appropriate. The upper surfaces are quite flat over most of the chord but rather over-optimised relative to the lower surfaces, and extensive rear loading is carried. This gives a trend to poor high-C_L performance at low Mach numbers and good high-C_L performance at higher Mach numbers, the converse of that required here. Finally, it should be pointed out that the Mach number penetration in cruise conditions is higher on actual operating propellers than would be expected from two-dimensional tests, although it is hoped and expected that the relative benefits would carry across.

The two sections described illustrate that the good performance of the 6 per cent thickness/chord section is maintained for other, widely varying, thicknesses. This continuity of performance has been found to apply over the whole ARA-D series of sections.

Profile coordinates of a selection of sections from the series, of thickness/chord ratio 6 per cent, 10 per cent, 13 per cent and 20 per cent, are presented in Table II.

5. Applications

Some of the potential and actual applications of the new sections so far considered can be summarised as follows.

A propeller has been designed for an aircraft project for which blade performance at 0.7 x radius is roughly in line with the data in Table I. It was found that the use of ARA-D series sections resulted in a potential 20 per cent increase in static thrust, when compared with NACA series 16 sections. This improvement was used to reduce the blade chord and thus effect a considerable weight saving.

TABLE II

ARA-D Section Ordinates

6% thickness/chord			10% thickness/chord			13% thickness/chord			20% thickness/chord		
x/c	z_{upper}/c	z_{lower}/c	x/c	z_{upper}/c	z_{lower}/c	x/c	z_{upper}/c	z_{lower}/c	x/c	z_{upper}/c	z_{lower}/c
0.0	0.0	0.0	0.0	0.0	0.0	0.0	0.0	0.0	0.0	0.0	0.0
0.003	0.009099	-0.004658	0.003	0.013713	-0.007388	0.003	0.016690	-0.008889	0.003	0.022030	-0.010575
0.01	0.017152	-0.007411	0.01	0.025227	-0.012555	0.01	0.030501	-0.015423	0.01	0.040200	-0.018816
0.02	0.024678	-0.008934	0.02	0.035554	-0.016369	0.02	0.042765	-0.020588	0.02	0.056441	-0.025912
0.04	0.035135	-0.009318	0.04	0.049237	-0.020033	0.04	0.058860	-0.026311	0.04	0.078139	-0.035093
0.07	0.045809	-0.007339	0.07	0.062305	-0.021626	0.07	0.074042	-0.030339	0.07	0.099311	-0.043996
0.10	0.053377	-0.004076	0.10	0.070856	-0.021088	0.10	0.083817	-0.031808	0.10	0.113559	-0.050022
0.15	0.062118	0.002198	0.15	0.079585	-0.018291	0.15	0.093428	-0.031723	0.15	0.128206	-0.056617
0.20	0.068235	0.007996	0.20	0.084614	-0.015159	0.20	0.098375	-0.030642	0.20	0.135379	-0.060487
0.25	0.072750	0.012750	0.25	0.087500	-0.012500	0.25	0.100531	-0.029469	0.25	0.137500	-0.062500
0.3	0.076067	0.016295	0.30	0.088908	-0.010571	0.30	0.100753	-0.028526	0.30	0.135846	-0.063102
0.35	0.078178	0.018834	0.35	0.088961	-0.009175	0.35	0.099332	-0.027687	0.35	0.131143	-0.062570
0.4	0.079022	0.020553	0.40	0.087685	-0.008108	0.40	0.096418	-0.026803	0.40	0.123961	-0.061087
0.45	0.078668	0.021539	0.45	0.085232	-0.007304	0.45	0.092257	-0.025845	0.45	0.115225	-0.058802
0.5	0.077173	0.021827	0.50	0.081734	-0.006734	0.50	0.087058	-0.024808	0.50	0.105825	-0.055825
0.55	0.074566	0.021435	0.55	0.077289	-0.006377	0.55	0.080985	-0.023686	0.55	0.096427	-0.052241
0.6	0.070912	0.020401	0.60	0.072014	-0.006214	0.60	0.074199	-0.022484	0.60	0.087114	-0.048148
0.65	0.066260	0.018750	0.65	0.066012	-0.006227	0.65	0.066848	-0.021206	0.65	0.077827	-0.043638
0.7	0.060628	0.016501	0.70	0.059363	-0.006399	0.70	0.059069	-0.019847	0.70	0.068516	-0.038802
0.75	0.054022	0.013723	0.75	0.052101	-0.006673	0.75	0.050964	-0.018382	0.75	0.059178	-0.033745
0.8	0.046416	0.010504	0.80	0.044232	-0.006965	0.80	0.042648	-0.016761	0.80	0.049830	-0.028597
0.85	0.037752	0.006940	0.85	0.035756	-0.007181	0.85	0.034252	-0.014930	0.85	0.040496	-0.023543
0.9	0.028002	0.003084	0.90	0.026692	-0.007282	0.90	0.025824	-0.012895	0.90	0.031165	-0.018788
0.95	0.017193	-0.001015	0.95	0.017146	-0.007282	0.95	0.017412	-0.010755	0.95	0.021832	-0.014762
0.975	0.011484	-0.003184	0.975	0.012327	-0.007338	0.975	0.013217	-0.009791	0.975	0.017175	-0.013306
1.0	0.005500	-0.005500	1.0	0.007500	-0.007500	1.0	0.009000	-0.009000	1.0	0.012500	-0.012500

A low-solidity ducted fan has been designed and tested. This is a reduced scale model of a cooling tower fan and operates at low rotational speeds. Use of the new sections was found to give high levels of efficiency at increased loading, giving roughly twice the performance of the blade with C-4 sections which had previously been tested. Thus a reduced number of blades or a smaller fan could have been used. Admittedly increased camber was involved, but this highlights the fact that the ARA-D series have optimised camber for a wide range of applications.

A new single-engined light aircraft is flying with a ducted fan integrated into the fuselage. In the near future, tests are to be conducted with fans incorporating the new sections and the effect of varying the number of blades will be established. It is expected that weight will be saved and performance improved.

Finally, there has been a recent revival of interest in turboprop airliners cruising at a Mach number approaching 0.8. The improved high Mach number penetration of the new sections could be utilised, with some modification to the very thick sections, particularly if higher blade loadings are required.

6. Concluding Remarks

Sections have been developed which, given the practical constraints, probably have a near optimum high-lift performance for a wide range of Mach numbers. This is combined with good Mach number penetration for the thinner sections. The sections are linked in a unique manner to give a profile distortion with thickness appropriate to the required aerodynamic performance at flow conditions likely for that thickness.

The section development has proceeded in a two-dimensional context, but the potential and actual applications suggest that the relative benefits carry across to the true situation of dynamic rotating flow. This certainly appears to be true of high-lift static conditions.

In general, the optimised performance of the present sections may be taken as a direct gain. More usually, size may be reduced for a given performance, with weight and cost benefits. The definition of a unique section profile of the basic family for a given thickness results in considerable simplification in blade design procedures. Furthermore, the likelihood of a non-optimum design is avoided.

Although a major feature of the sections is the favourable supercritical flow development, the section geometries are dissimilar in many respects to aircraft wing "supercritical" sections by virtue of different design conditions and practical constraints. Incidentally, shape changes due to manufacturing inaccuracies, etc, in important surface regions where supercritical flow is anticipated, are expected not to have a disproportionate influence. Also, the flow development is such as to encourage extensive laminar regions in many situations. Of course, in practice leading-edge guards may be fitted and surfaces roughened or corroded, which would tend to fix forward transition to turbulent flow. Experimental tests have shown a relative insensitivity to such factors, except in flow conditions which are unlikely to arise in practice.

References

1	—	SBAC Standard Method of Propeller Performance Estimation.
2	H Glauert	*The Elements of Aerofoil and Airscrew Theory.* Cambridge University Press, 1947.
3	F Bauer P Garabedian D Korn	A theory of supercritical wing sections, with computer programs and examples. Lecture Notes in Economics and Mathematical Systems, No 66, Springer, 1972.
4	C C L Sells	Plane subcritical flow past a lifting aerofoil. RAE Technical Report 67146, 1967.
5	B J Powell	Calculation of the pressure distribution on a thick cambered aerofoil at subsonic speeds, including the effects of the boundary layer. NPL Aero Report 1238, 1967.
6	H P Horton	The calculation of the compressible turbulent boundary layer by the entrainment history method. Hawker Siddeley Aviation, HSA/Hatfield/Research/1048/HPH, 1969.